

## 1. INTRODUCTION

Moisture transport in the atmosphere is one of the most significant components in the hydrological cycle. Under stationary condition, ocean surface fresh water flux, which is the difference between precipitation (P) and evaporation (E), is balanced by the divergence of column-integrated moisture transport (IMT) in the atmosphere. Characterizing accurately a global picture of IMT from observation is a difficult task. It requires measurements of vertical profiles for wind vector and humidity. More specifically, IMT can be defined as the integration in pressure coordinates the product of specific humidity  $q$  and wind vector  $\mathbf{u}$ ,

$$\mathbf{IMT} = \frac{1}{g} \int_0^{p_s} \mathbf{u} q dp \quad (1)$$

where  $g$  is the gravitational acceleration, and  $p_s$  is the atmospheric pressure at ocean surface. Traditionally, vertical profiles come from aerological (radiosonde) data. Over oceans, radiosonde data are sparse. Liu (1993) proposed a method to estimate IMT, using surface wind vector  $\mathbf{u}_s$  measured by the scatterometer and the vertically integrated water vapor ( $W$ ) measured by microwave radiometer. The method uses an equivalent velocity  $\mathbf{u}_e$  defined by

$$\mathbf{u}_e = \mathbf{IMT} / W \quad (2)$$

where,

$$W = \frac{1}{g} \int_0^{p_s} q dp \quad (3)$$

is the column-integrated water vapor. The equivalent velocity  $\mathbf{u}_e$  is basically a depth-averaged velocity weighted by the humidity. Since  $W$  can be accurately measured by both the operational spacebased microwave radiometers such as SSM/I and TMI, the problem of measuring

IMT is essentially the determination of  $\mathbf{u}_e$ . The variability of humidity profile has been extensively studied by Liu et al. (1991) and the dominant mode of variability was found to peak at the top of the boundary layer. Heta and Mitsuta (1993), using  $W$  derived by Liu (1987) from the microwave radiometer on Nimbus-7 and using 850 mb cloud drift winds as  $\mathbf{u}_e$ , have satisfactorily estimated E-P in the tropical Pacific. The top of the boundary layer is approximately at 850mb and wind at this level is closely related to surface level wind through similarity relations (e.g., Brown and Liu,

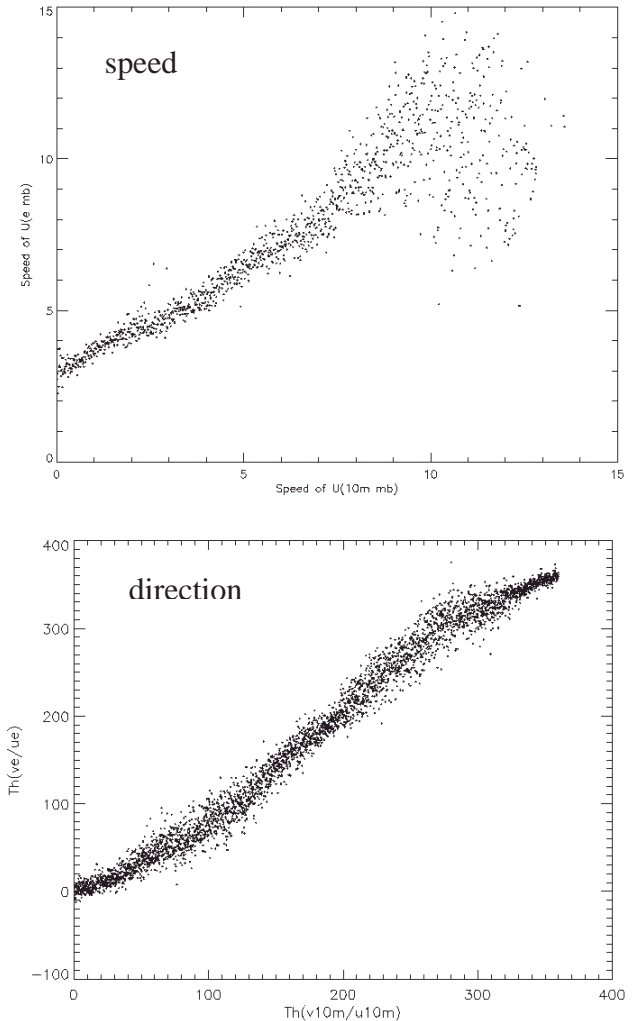


Figure 1. Relation between the equivalent velocity for moisture transport and the 10m-wind velocity, derived from NCEP reanalysis data.

---

Corresponding author address:

Wenqing Tang, Jet Propulsion Laboratory,  
California Institute of Technology, MS 300-  
323, Pasadena, CA 91109; e-mail:  
wqt@pacific.jpl.nasa.gov

1982). In the past, oceanographers used to get ocean surface wind stress by multiply in the geostrophic winds (derived from pressure gradient) by a constant factor and turning them by a constant angle. Figure 1 shows the close relation between  $u_e$  and  $u_s$  derived using data from the National Centers for Environmental Prediction (NCEP) reanalysis project. Spaceborne scatterometer could measure surface wind vector  $u_s$  over global ocean. In this study, a statistical relationship is derived between  $u_e$  and  $u_s$  using data from numerical weather prediction model. The relationship is then validated using surface and vertical profile from radiosonde data, before applied to spacebased measurements.

## 2. MODEL AND VALIDATION

We first derived the statistical relation between surface wind velocity  $u_s$  and the equivalent velocity for moisture transport  $u_e$  using data from NCEP reanalysis project. The datasets is 6-hourly (0, 6, 12 and 18Z) over global oceans at 2.5x2.5 degree horizontal resolution and 17 vertical pressure levels from 1000mb to 10mb on a complete set of geophysical variables. Parameters needed for this study include the surface wind components at 10m, vertical profiles of wind vector and specific humidity at pressure levels from 1000mb to 300mb. Only data between latitude of 60S and 60N were used. The equivalent velocity  $u_e$  is calculated at each grid point according to

formula (1-3) for each instantaneous map. Two kinds of averaging scheme were then applied to each component: monthly average and bin-average. Monthly average was obtained by simply averaging the instantaneous fields for the corresponding month. Bin-average is done by at first sub sampling surface wind component in the 0.1 m/s bin in the wind range from -20 m/s to 20 m/s, then calculating simple average of equivalent wind associated with each sub-sample bin. Multi-linear regression was performed on various ensembles: instantaneous, monthly averaged, and bin-averaged. In this report, we will focus on model function  $u_e' = F(u_s)$  derived on instantaneous ensembles, with linear regression for zonal component as  $2.045+1.422x$ , and for meridional component as  $0.014+0.718x$ .

Radiosonde data were used to validate such derived relation between  $u_s$  and  $u_e$ . Measured  $u_e$  were obtained from humidity weighted integration on the vertical profile of wind and dew point temperature, which were converted to specific humidity, as shown in formula (1-3). A quality control process was in place to select  $u_e$  for validation only if there exist 5 or more measurements at pressure levels between 1000mb and 300mb. Surface wind measurements are also available for most radiosonde records, but at various sensor height for various stations. Therefore radiosonde measured  $u_s$  were converted to 10m equivalent neutral wind using algorithm described in Liu and Tang (1996), in

Table 1. Results on statistical comparison between  $u_e$  (measured) and  $u_e'$  (derived from  $u_s$ ) on radiosonde stations.

Location		N	Zonal Comp.			Merid. Comp.		
			Corr.	mean	Std.Dev.	Corr.	mean	Std.Dev.
130.58E	31.63N	1118	0.56	1.86	4.23	0.63	-1.45	4.34
72.40E	7.30S	290	0.87	-1.03	3.05	0.73	-0.14	1.81
131.23E	25.83N	1365	0.6	2.82	4.1	0.85	-1.06	3.15
141.33E	24.78N	1303	0.44	2.73	4.97	0.5	-1.42	3.43
167.73E	8.73N	1128	0.78	0.28	2.3	0.73	-1.12	1.48
73.15E	8.3N	260	0.71	-2.24	3.05	0.62	1.16	2.24
55.53E	4.68S	940	0.62	1.01	4.18	0.76	-1.38	2.32
77.53E	37.8S	85	0.65	0.34	3.88	0.67	0.46	3.72
172.92E	1.35N	333	0.6	-1.04	2.49	0.61	1.16	1.58
179.22E	8.52S	368	0.71	-0.38	3.12	0.73	0.88	1.7
170.72W	14.33S	1145	0.71	0.87	3.77	0.71	0.73	1.81
170.22W	57.15S	711	0.77	0.55	4.3	0.87	-0.33	4.12
171.38E	7.08N	790	0.72	-0.79	2.64	0.63	-0.36	1.34
29.32W	20.50S	174	0.67	-1.45	2.72	0.79	0.98	2.8

order to be consistent with scatterometer measurement and the model function. Finally, model function  $\mathbf{u}_e' = \mathbf{F}(\mathbf{u}_s)$  were applied to  $\mathbf{u}_s$  to obtain surface wind derived equivalent wind velocity  $\mathbf{u}_e'$ . Statistical comparison were performed between radiosonde  $\mathbf{u}_e$  and  $\mathbf{u}_e'$ , and results are shown in Table 1. Results at all stations show positive and significant correlation between  $\mathbf{u}_e$  and  $\mathbf{u}_e'$ , with mean difference less than 3m/s. The standard deviation for zonal component is higher than that for meridional component. Further work is needed to identify the error sources and lead to improvement on the model function.

### 3. SPACEDBASED MOISTURE ADVECTION

Data from two spacebased missions, SeaWinds on QuikSCAT and TMI on TRMM, were combined to derive atmosphere moisture transport fields over the oceans. QuikSCAT launched by NASA in

July 1999 is a Ku-band (14 GHz) scatterometer with pencil-beam antennas in a conical scan. It measures backscatter sigma0, from which oceans surface winds were retrieved, at resolution of 25km along a swath of 1800km wide, and covers global ocean 93% in 24 hours. In comparison with buoy measurements, QuikSCAT was found with rms difference of 0.7 m/s in speed and 13° in direction for over 5000 collocated measurements (Wentz, 2001). Objectively interpolated global wind fields on uniform grids have been produced at 0.5 degree resolution, twice daily. Liu et al (1998) demonstrated that scatterometer reveals more detailed structure of the global wind fields than operational numerical weather prediction (NWP) products.

TRMM, a joint mission of NASA and the National Space Development Agency (NASDA) of Japan, was launched in November 1997. The Microwave

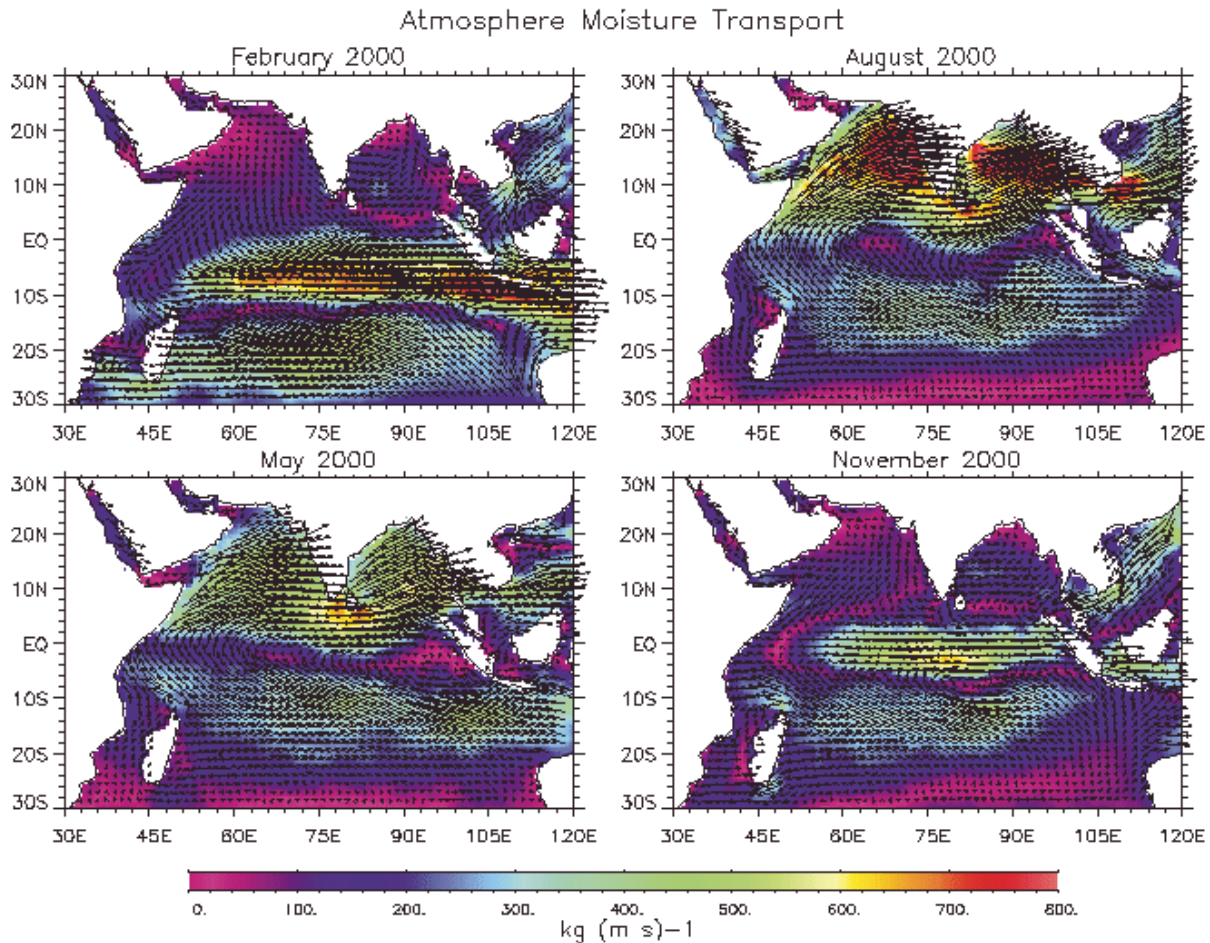


Figure 2. Atmospheric moisture transport derived from combined missions of QuikSCAT and TRMM in Indian Ocean for February, May, August and November 2000.

Imager (TMI) on board of TRMM measures radiance from 10.7 GHz to 85 GHz, from which a suite of parameters can be derived, including sea surface temperature, surface wind speed, integrated water vapor and rainfall over ocean. Daily maps of integrated water vapor used in this study are obtained from Remote Sensing System. Integrated water vapor is also available from measurement by Special Sensing Microwave / Imager (SSM/I) since 1987, with a much longer history. TRMM/TMI was chosen for more comprehensive study using TRMM measured precipitation.

Spacebased moisture advection was obtained by applying the model function for equivalent velocity to the surface wind vector fields measured by

QuikSCAT and multiplied with integrated water vapor  $W$  measured by TMI. Figure 2 shows the moisture transport over Indian Ocean for February, May, August and November in 2000. It reveals a complete picture of moisture transport for the various stages of Indian monsoon.

Figure 3 shows a time series of moisture transport from Atlantic Ocean along three sections on the South America east coast; integrated surface rain-rate measured by TRMM for Amazon area is also plotted for comparison. It is to demonstrate that with the accuracy, coverage and resolution of spacebased measurements, we can quantitatively analyze the moisture transport from the oceans to the continents of interest, and to study various processes governing oceanic influence of

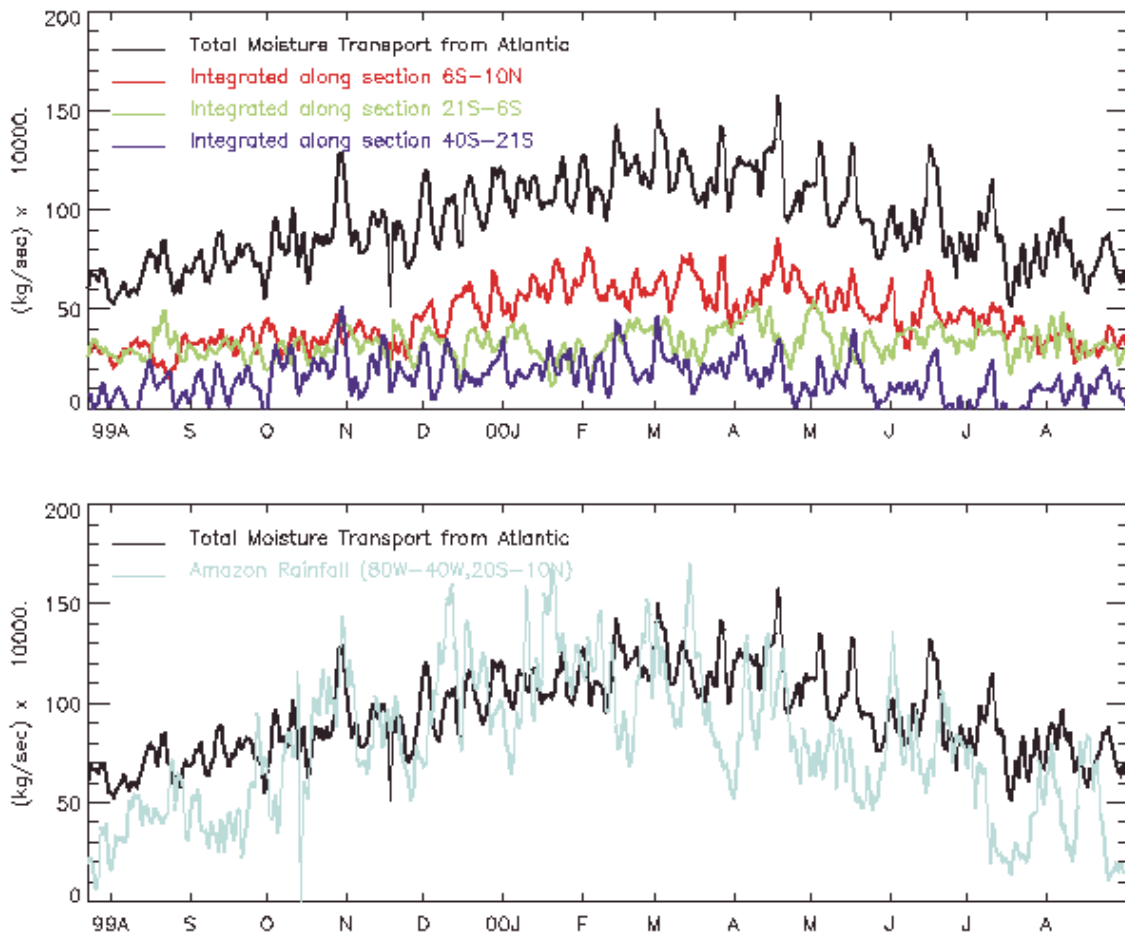


Figure 3. (upper) Moisture transport from Atlantic Ocean integrated along three coastal sections is plotted in red (6S-10N), green (21S-6S), and blue (40S-21S), respectively. Total of three sections is plotted in black. (lower) Total moisture transport from Atlantic Ocean is compared with rain rate in Amazon area (80W-40W, 20S-10N, land).

continental hydrologic balance, which might have significant economical impact to society.

#### REFERENCE

Brown, R.A., and W. T. Liu, 1982: An operational large-scale marine planetary boundary layer model, *J. Appl. Meteor.*, 2, 261-269.

Heta, Y. and Y. Mitsuta, 1993: An evaluation of evaporation over the tropical Pacific Ocean as observed from satellites, *J. Appl. Meteor.*, 32, 1242-1247.

Liu, W. T., W. Tang, and P. S. Polito, 1998: NASA scatterometer provides global ocean-surface wind fields with more structures than numerical weather prediction. *Geophys. Res. Lett.*, 25, 761-764.

Liu, W. T., and W. Tang, 1996: Equivalent Neutral Wind, JPL Publi, 96-17, Jet Propulsion Laboratory, Pasadena, California, 16pp.

Liu, W. T., 1993: Ocean Surface Evaporation. Atlas of Satellite Observations Related to Global Change, R.J. Gurney, J. Foster, and C. Parkinson (eds.), Cambridge University Press, Cambridge, 265-278.

Liu, W. T., 1991: W. Tang, and P. P. Niiler, 1991: Humidity profiles over ocean, *J. Climate*, 4, 1023-1034.

Wentz, F. D. Smith, and C. Mears, 2001: Advanced Algorithm for QuikSCAT and SeaWinds/AMSR, Proc. Of IGARSS 2001, IEEE, in press.